Research in Astron. Astrophys. **2011** Vol. **11** No. **9**, 1003–1018
*http://www.raa-journal.org* *http://www.iop.org/journals/raa*

*Research in Astronomy and Astrophysics*

# The effects of BCGs on the statistics of large-separation lensed quasars by clusters *

Hong Qi and Da-Ming Chen

National Astronomical Observatories, Chinese Academy of Sciences, Beijing 100012, China; *hongqi@bao.ac.cn; cdm@bao.ac.cn*

Received 2011 April 13; accepted 2011 May 15

**Abstract** We study the statistics of large-separation multiply-imaged quasars lensed by clusters of galaxies. In particular, we examine how the observed brightest cluster galaxies (BCGs) affect the predicted numbers of wide-separation lenses. We model the lens as an NFW-profiled dark matter halo with a truncated singular isothermal sphere to represent the BCG in its center. We mainly make predictions for the Sloan Digital Sky Survey Quasar Lens Search (SQLS) sample from the Data Release 5 (DR5) in two standard $\Lambda$CDM cosmological models: a model with matter density $\Omega_{\rm M} = 0.3$ and $\sigma_8 = 0.9$, as is usually adopted in the literature ($\Lambda$CDM1), and a model suggested by the WMAP seven-year (WMAP7) data with $\Omega_{\rm M} = 0.266$ and $\sigma_8 = 0.801$. We also study the lensing properties for the WMAP3 cosmology in order to compare with the previous work. We find that BCGs in the centers of clusters significantly enhance the lensing efficiency by a factor of $2 \sim 3$ compared with that of NFW-profiled pure dark matter halos. In addition, the dependence of mass ratios of BCGs to their host halos on the host halo masses reduces the lensing rate by $\sim 20\%$ from assuming a constant ratio as in previous studies, but considering the evolution of this ratio with redshift out to $z \sim 1$ would reduce it by $\sim 3\%$. Moreover, we predict that the numbers of lensed quasars with image separations larger than $10''$ in the statistical sample of SQLS from DR5 are $1.22$ and $0.47$, respectively for $\Lambda$CDM1 and WMAP7 and $0.73$ and $0.33$ for separations between $10''$ and $20''$, which are consistent with the only observed cluster lens with such a large separation in the complete SQLS sample.

**Key words:** cosmological parameters — cosmology: theory — galaxies: clusters — gravitational lensing — dark matter

## 1 INTRODUCTION

Clusters of galaxies provide some of the most spectacular examples of gravitational lensing. Theoretical work was performed even before the discovery of QSO 0957+561 (Walsh et al. 1979). Cluster lensing entered the observational realm with the discovery of giant blue luminous arcs representing the images of background galaxies (Paczynski 1987) in the clusters A 370 and Cl 2244 (Soucail et al. 1987; Lynds & Petrosian 1986). So far, hundreds of arcs lensed by clusters have been confirmed. However, the search for multiply-imaged quasars by clusters of galaxies has been less

* Supported by the National Natural Science Foundation of China.

successful. The number of quasars lensed by galaxies has reached roughly $150$ now and the typical image separation of these systems ranges from $0.3''$ to $7''$ (Li et al. 2007). Lensing of quasars by clusters of galaxies was finally observed with the discovery and confirmation of SDSS J1004+4112 with an image separation of $14.7''$ found in the Sloan Digital Sky Survey (SDSS) (Inada et al. 2003; Oguri & Keeton 2004). By now two quasar lenses by clusters have been discovered from the spectroscopically confirmed quasars in the SDSS data. The other case was SDSS J1029+2623 with a separation of $22.5''$ (Inada et al. 2006).

The statistics of strong gravitational lensing can be used to constrain the density profile of dark matter halos (Keeton & Madau 2001; Wyithe et al. 2001; Takahashi & Chiba 2001; Li & Ostriker 2002; Oguri et al. 2002; Huterer & Ma 2004; Kuhlen et al. 2004; Hennawi et al. 2007b; Li et al. 2007), the abundance of massive dark matter halos (Narayan & White 1988; Wambsganss et al. 1995; Kochanek 1995; Nakamura & Suto 1997; Mortlock & Webster 2000a; Lopes & Miller 2004; Chen 2004; Oguri & Keeton 2004; Hennawi et al. 2007a; Li et al. 2007; Li & Chen 2009), or cosmological parameters (Mortlock & Webster 2000b; Mitchell et al. 2005). Those aspects have been studied using giant arc statistics where the sources were galaxies (Bartelmann et al. 1998; Oguri et al. 2003). The analysis of the statistics of lensed quasars and that of giant arcs in fact complement each other in several ways (see Oguri & Keeton 2004, for more details). Although there are many examples of galaxies lensed by clusters, large-separation lensed quasars have several advantages over arcs as a cosmological probe (Inada et al. 2006). First, the point-like structure of quasars and their well-understood redshift distribution can make the large-separation lensed quasars much cleaner probes of cosmology and structure formation models (e.g., Oguri & Keeton 2004; Hennawi et al. 2007a), while the statistics of arcs remain contentious (Bartelmann et al. 2003). Secondly, the time-variability of quasars allows the measurement of time-delays among the multiple lensed images, thereby giving a priori knowledge of the Hubble constant (e.g., Kochanek 2002). In this paper, we use quasars as lensed sources to study the properties of gravitational lensing by clusters of galaxies.

The mass density profile of clusters has been a debated topic. Although a typical value for the inner slopes of clusters ranges from $0.7$ to $1.5$ (Schmidt & Allen 2007), the inner slope $\alpha$ and the concentration $c_{\rm vir}$ have been particularly controversial, with different groups obtaining totally contrary results even for the same clusters (e.g., Bullock et al. 2001; Broadhurst et al. 2005; Smith et al. 2005; Gavazzi et al. 2005; Zappacosta et al. 2006; Schmidt & Allen 2007; Umetsu & Broadhurst 2008; Bradač et al. 2008; Tu et al. 2008; Limousin et al. 2008; Newman et al. 2009). In addition, the stellar mass of the central galaxy is often neglected since it is regarded as a negligible contribution to the total mass. However, this is not the case in the innermost region where the gravitational potential is dominated by baryons (Ahn et al. 2007).

A number of studies made predictions of the abundance of large-separation lensed quasars by dark matter halos on cluster scales. Oguri & Keeton (2004) pointed out that the triaxiality of dark matter halos systematically enhanced the lensing probability by a factor of $2 \sim 4$, assuming dark matter halos with NFW density profiles. In addition, the inner structures of dark matter halos were proposed to be modified by introducing baryonic cooling and compression (Porciani & Madau 2001; Kochanek & White 2000; Sarbu et al. 2001; Oguri et al. 2002; Chen 2003b,a; Bowman et al. 2004). Some studies involved supermassive black holes (SMBHs) at the centers of galaxies to explain the influence of baryons on gravtitational lensing (e.g., Mao et al. 2001; Chen 2003b,a; Ahn et al. 2007). Recent observations show that very luminous galaxies reside in the deep potential wells of clusters of galaxies and several groups (Hennawi et al. 2007b; Li et al. 2007; Sommer-Larsen & Limousin 2010) adopted numerical simulation methods to account for the effects of such brightest cluster galaxies (BCGs) and demonstrated that the introduction of BCGs to dark matter halos increased the lensing probabilities by $\sim 50\%$. Hennawi et al. (2007b) and Li et al. (2007) regarded the mass ratio of BCGs to their host halos to be a fixed value for simplification. In this paper, we discuss in detail the effects of BCGs on lensing efficiency and compare the predicted numbers of large-separation lensed quasars as a function of image separation in three cosmological models.

The remainder of this paper is organized as follows. In Section 2 we describe the basic formulism of gravitational lensing. In Section 3 we give the overall results of our work. In Section 4 we present discussions. In this paper we adopt three cosmologies: the popular concordance cosmology with $\Omega_{\rm M} = 0.3$, $\Omega_\Lambda = 0.7$, $\sigma_8 = 0.9$ and $h = 0.7$ ($\Lambda$CDM1), the cosmology favored by the seven-year Wilkinson Microwave Anisotropy Probe (WMAP) observations with $\Omega_{\rm M} = 0.266$, $\Omega_\Lambda = 0.734$, $\sigma_8 = 0.801$ and $h = 0.71$ (WMAP7) and also the WMAP3 cosmology with $\Omega_{\rm M} = 0.238$, $\Omega_\Lambda = 0.762$, $\sigma_8 = 0.74$ and $h = 0.73$ in order to compare with Li et al. (2007).

## 2 LENSING BASICS

### 2.1 Therectical Model and Lensing Equations

The lensing probability is extremely sensitive to the mass density profile of the lens, which is characterized by the inner density slope $\alpha$. In previous work the inner slope was modified by introducing a BCG in the center of a cluster and Hennawi et al. (2007b) quantified the effect of BCGs on cluster lensing efficiency under the assumption that the mass ratio of BCGs to their host halos was a constant value. However, since lensing rate is very sensitive to the inner density slope, we should carefully handle BCGs which occupy the innermost region of clusters.

We place a BCG in the potential center of each cluster and assume the correlation between the mass of BCGs to that of their host halos follows the relationship (Wang & Jing 2010)

$$M_{\rm b} = \frac{2}{\left(\frac{M}{M_0}\right)^{-\alpha} + \left(\frac{M}{M_0}\right)^{-\beta}} \times k, \tag{1}$$

where $M_{\rm b}$ is the mass of the BCG and $M$ is the mass of the host dark matter halo. $M_0$, $\alpha$, $\beta$ and $k$ are parameters. The best fit model to the SDSS observation has the following parameters: $M_0 = 4 \times 10^{11}\ h^{-1}\ M_\odot$, $\alpha = 0.29$, $\beta = 2.42$ and $\log k = 10.35$. We also consider the evolution of mass ratios of BCGs to their host halos with redshift by assuming the double power law form as described in Equation (1) and that the host mass $M$ and the corresponding parameter $k$ evolve with time linearly (Wang & Jing 2010). The model has parameters $M_0 = 3.21 \times 10^{11}\ h^{-1}\ M_\odot$, $\log k = 10.17$ at redshift $z = 0$ and $M_0 = 4.34 \times 10^{11}\ h^{-1}\ M_\odot$, $\log k = 10.15$ at redshift $z = 0.83$. For halos at redshifts larger than $0.83$, we assume the same mass ratio relationship as that at redshift $0.83$. The scatter of the mass of BCGs, $M_{\rm b}$, at a given mass $M$ of their host halos was described with a Gaussian function, but for simplification we do not consider the distribution.

Baryonic effects should be substantially weaker in galaxy clusters than in galaxies and density profiles outside the innermost cores should still reflect those of typical CDM halos found in numerical simulations (Comerford et al. 2006). Therefore, the BCG is modeled as a truncated singular isothermal sphere (SIS), which accurately represents strong lensing by an elliptical galaxy (Hennawi et al. 2007a), with a mass density

$$\rho(r) = \frac{{\sigma_{\rm v}}^2}{2\pi G}\frac{1}{r^2}, \tag{2}$$

where $\sigma_{\rm v}$ is the velocity dispersion (Turner et al. 1984). In the absence of a theory of BCG formation, we scale the velocity dispersions of BCGs with the masses of dark matter halos. Normalizing this relationship to the Coma cluster gives (Hennawi et al. 2007b)

$$\frac{\sigma_{\rm v}}{300\ {\rm km\ s^{-1}}} = \left(\frac{M}{10^{15} M_\odot}\right)^{\frac{2}{15}}, \tag{3}$$

where $M$ is the mass of the host dark matter halo.

The truncation radius is given by Hennawi et al. (2007b)

$$r_{\rm max} = \frac{GM_{\rm b}}{2{\sigma_{\rm v}}^2}. \tag{4}$$

We model the cluster component as an NFW profile which was proposed in cosmological N-body simulations (Navarro et al. 1997) with a mass density

$$\rho(r) = \frac{\rho_{\rm s}{r_{\rm s}}^3}{r\left(r+r_{\rm s}\right)^2}, \tag{5}$$

where $\rho_{\rm s}$ and $r_{\rm s}$ are constant with respect to radius. Here $r_{\rm s}$ is the scaled radius of the dark matter halo which is also used as the length scale in the lens plane.

For a dark matter halo with an NFW profile, its mass diverges logarithmically as $r \rightarrow \infty$. We define the mass of a halo to be the mass inside a sphere within which the average mass density is $\delta_{\rm vir}$ times the critical density $\rho_{\rm crit}$ of the universe. Correspondingly, $r_{\rm vir}$ is the virial radius defined as the radius of a sphere at which the average density interior to it is greater than or equal to $\delta_{\rm vir}$ times $\rho_{\rm crit}$ and we obtain (see Navarro et al. 1997; Li & Ostriker 2002)

$$\rho_{\rm s} = \frac{\delta_{\rm vir}}{3}\rho_{\rm crit,0}\left[\Omega_M(1+z)^3+\Omega_\Lambda\right]\frac{{c_{\rm vir}}^3}{f(c_{\rm vir})}, \tag{6}$$

and

$$r_{\rm s} = \frac{1}{c_{\rm vir}}\left(\frac{3M}{4\pi\delta_{\rm vir}\rho_{\rm crit,0}\left[\Omega_M(1+z)^3+\Omega_\Lambda\right]}\right)^{\frac{1}{3}}, \tag{7}$$

where $c_{\rm vir} = r_{\rm vir}/r_{\rm s}$ is the concentration parameter and $f(c_{\rm vir}) = \ln(1+c_{\rm vir}) - c_{\rm vir}/(1+c_{\rm vir})$. Once we know the concentration parameter, $c_{\rm vir}$, $\rho_{\rm s}$ and $r_{\rm s}$ can be determined for a halo with mass $M$.

The lensing selected cluster samples are likely to show significant concentration bias (Hennawi et al. 2004). Since the cross section is a steep function of cluster mass, it is desirable to first normalize out the mass dependence of cluster concentration. Thus we should consider the distribution of $c_{\rm vir}/c_{\rm vir}(M)$, where $c_{\rm vir}(M)$ is the median concentration parameter and the virial overdensity is $\delta_{\rm vir}(z) \approx (18\pi^2 + 82x - 39x^2)/(1+x)$ , with $x \equiv \Omega_M(z) - 1$ (Hennawi et al. 2007b). In practice, we do not implement this distribution but assume that all halos with the same masses have the median concentration parameter. In addition, the mass concentration should decline with increasing cluster mass because in the hierarchical model massive clusters form later, when the cosmological background density is lower. We adopt a fitting formula given by Hennawi et al. (2007a):

$$c_{\rm vir}(M) = \frac{12.3}{1+z}\left(\frac{M}{M_*}\right)^{-0.13}, \tag{8}$$

where $M_* = 1.3\times10^{13}\ h^{-1}\ M_\odot$ is the nonlinear mass at $z=0$ for our cosmologies.

The total surface mass density for an NFW halo with a BCG in its gravitational potential center can be calculated analytically

$$\Sigma(\boldsymbol{x}) = \Sigma_{\rm DM}(\boldsymbol{x}) + \Sigma_{\rm BCG}(\boldsymbol{x}), \tag{9}$$

where $\boldsymbol{x} = \boldsymbol{\xi}/r_{\rm s}$ is the dimensionless position vector of a point in the lens plane and $\boldsymbol{\xi}$ is the physical position vector in the lens plane. As the density profile of the lens model is spherical, we can use $x = |\boldsymbol{x}|$ to take the place of $\boldsymbol{x}$ in Equation (9). $\Sigma_{\rm DM}(x)$ is the surface mass density of the NFW-profiled dark matter halo and $\Sigma_{\rm BCG}(x)$ is that of the center BCG, given by Li & Ostriker (2002)

$$\Sigma_{\rm DM}(x) = 2\rho_{\rm s}r_{\rm s}\int_0^\infty \left(x^2+z^2\right)^{-\frac{1}{2}}\left[(x^2+z^2)^{\frac{1}{2}}+1\right]^{-2}dz, \tag{10}$$

and

$$\Sigma_{\rm BCG}(x) = \frac{{\sigma_{\rm v}}^2}{\pi G r_{\rm s} x} \arctan \frac{r_{\rm max}}{r_{\rm s} x}, |x| \leq \frac{r_{\rm max}}{r_{\rm s}}. \tag{11}$$

The lensing equation is given by

$$y = x - \frac{\alpha(x)}{x}\,, \tag{12}$$

where $y = |\boldsymbol{y}|$ and $\boldsymbol{y} = \boldsymbol{\eta}/(r_{\rm s} D_{\rm S}^{\rm A}/D_{\rm L}^{\rm A})$ is the dimensionless position vector of a point in the source plane. $D_{\rm S}^{\rm A}$ and $D_{\rm L}^{\rm A}$ are the angular diameter distance between the source and the observer and between the lens and the observer, respectively. Correspondingly, $\eta = |\boldsymbol{\eta}|$, with $\boldsymbol{\eta}$ being the physical position vector in the source plane and

$$\alpha(x) \equiv 2 \int_0^x \frac{\Sigma(x')}{\Sigma_{\rm cr}} x' dx'\,, \tag{13}$$

where $\Sigma_{\rm cr}$ is the critical surface mass density defined by (Turner et al. 1984)

$$\Sigma_{\rm cr} \equiv \frac{c^2}{4\pi G} \frac{D_{\rm S}^{\rm A}}{D_{\rm L}^{\rm A} D_{\rm LS}^{\rm A}}, \tag{14}$$

where $D_{\rm LS}^{\rm A}$ is the angular diameter distance between the lens and the source. Note that $D_{\rm S}^{\rm A} \neq D_{\rm L}^{\rm A} + D_{\rm LS}^{\rm A}$.

Inserting Equations (9), (10) and (11) into Equation (13), we obtain the lensing equation for this NFW+BCG density profile lens model

$$y = x - \frac{\mu_{\rm s} g(x) + \alpha_{\rm b}(x)}{x}, \tag{15}$$

where $\mu_{\rm s}$ represents the strength of an NFW halo to produce multiple images and is defined by Li & Ostriker (2002)

$$\mu_{\rm s} \equiv \frac{4\rho_{\rm s} r_{\rm s}}{\Sigma_{\rm cr}}, \tag{16}$$

and $g(x)$ is given by Bartelmann et al. (1998)

$$g(x) \equiv \ln \frac{x}{2} + \begin{cases} \frac{1}{\sqrt{x^2-1}} \arctan \sqrt{x^2-1} & (x > 1)\,, \\ 1 & (x = 1)\,, \\ \frac{1}{\sqrt{1-x^2}} \arctan h \sqrt{1-x^2} & (0 < x < 1)\,. \end{cases} \tag{17}$$

The function $\alpha_{\rm b}(x)$ is given by

$$\alpha_{\rm b}(x) = \frac{2\xi_0}{r_{\rm s}\pi} \int_0^x \arctan \frac{r_{\rm max}}{r_{\rm s} x'} dx', \tag{18}$$

where $\xi_0$ is defined as

$$\xi_0 = 4\pi \left(\frac{\sigma_{\rm v}}{c}\right)^2 \frac{D_{\rm L}^{\rm A} D_{\rm LS}^{\rm A}}{D_{\rm S}^{\rm A}}, \tag{19}$$

and note that from Equations (14) and (19) we have

$$\xi_0 = \frac{{\sigma_{\rm v}}^2}{G\Sigma_{\rm cr}}. \tag{20}$$

Multiple images are formed if and only if the sources are within the caustics, namely, $|y| \leq y_{\rm cr}$, where $y_{\rm cr} = |y(x_{\rm cr})|$; $x_{\rm cr} > 0$ is determined by $dy/dx = 0$. For each set of images, we define

the dimensionless image separation $\theta$ to be the maximum separation between any pair of images. This is a convenient definition that depends only on observable quantities and is well defined for all image configurations. In our case, image separation is treated as the splitting of two outer images. When $|y| < y_{\rm cr}$, there are three real roots of the lensing equation: $x_1 > x_2 > x_3$ and $\theta = r_{\rm s}\Delta x/D_{\rm L}^{\rm A}$, where $\Delta x = x_1 - x_3$. The value of $\Delta x$ is insensitive to the value of $y$ when $|y| < y_{\rm cr}$. So in practice, we can use $\Delta x = 2x_0$, where $x_0$ is the positive root of $y(x) = 0$. Then for a lens with mass $M$ at redshift $z$, the cross section in the lens plane for image separation $\theta > \theta_0$ is

$$\sigma(\,\theta; M, z) \approx \pi y_{\rm cr}^2 r_{\rm s}^2, \tag{21}$$

where the image separation is given by

$$\theta \approx \frac{2x_0 r_{\rm s}}{D_{\rm L}^{\rm A}}. \tag{22}$$

### 2.2 Magnification Bias and SQLS Sample

The magnification bias is one of the most important elements in predicting lensing probabilities. We must take a proper account of the effect of lensing biases (Turner et al. 1984; Kochanek 1995; Oguri & Keeton 2004) to compare theories with observations. According to Oguri & Keeton (2004), we not only count the sources but also weight them appropriately and the biased cross section can be written as

$$B\sigma = \int dX dY \frac{\phi(L/\mu)}{\phi(L)} \frac{1}{\mu}, \tag{23}$$

where the integral is over the multiply-imaged region of the source plane. Here $\mu$ is the magnification which can be chosen as total image magnification or the magnification of the fainter or brighter image depending on the observational quasar selection criteria and $\phi(L)$ is the luminosity function of source quasars. $X$ and $Y$ are dimensionless coordinates on the source plane.

Statistical analysis of lensed quasars requires a large well-defined lens sample that is selected from a well-understood source population since strong lensing probabilities are very sensitive to the volume from the source to the observer. We adopt the latest SDSS Quasar Lens Search (SQLS) for the strongly lensed quasars statistical sample, which was constructed from spectroscopically confirmed quasars in the SDSS Data Release 5 (DR5). Out of $77\,429$ quasars in DR5, the complete sample consists of $36\,287$ quasars which are located in the redshift range $0.6 < z_{\rm s} < 2.2$ and are brighter than the Galactic extinction corrected $i$-band magnitude of $19.1$. A statistical sample of $19$ lensed quasars was derived at image separations between $1''$ and $20''$ and $i$-band magnitude differences between the two lensed images were smaller than $1.25$ magnitude, which is larger than $10^{-0.5}$ in terms of flux ratios of faint to bright lensed images. Eighteen of these lenses are galaxy-scale lenses and one is a large separation ($14.7''$) system which is produced by a massive cluster of galaxies. In addition, the Data Release $5$ spectroscopic quasars contain $17$ additional lensed quasars outside the complete SQLS sample.

In order to match the selection function of the SQLS lensed quasar sample, the integral in Equation (23) is performed over the region where the flux ratio of faint to bright images is larger than $10^{-0.5}$ (Oguri et al. 2008). With the increasing number of high redshift quasars that were discovered in surveys with well-defined selection criteria, evidence was also found that the strong power-law evolution did not continue beyond source redshift $z_{\rm s} \sim 2$ (Boyle et al. 2000). Thus we adopt the double power law luminosity function constrained from the combination of the SDSS and 2dF (2SLAQ), namely the 2SLAQ+Croom et al. (2004) model in Richards et al. (2005) as our fiducial model (Oguri et al. 2008)

$$\phi(M_g) = \frac{\phi_*}{10^{0.4(1-\beta_{\rm h})(M_g - M_g^*)} + 10^{0.4(1-\beta_{\rm l})(M_g - M_g^*)}}, \tag{24}$$

$$M_g^*(z) = M_g^*(0) - 2.5(k_1 z + k_2 z^2), \tag{25}$$

with the parameters of ($\beta_{\rm h}$, $\beta_{\rm l}$, $\phi_*$, $M_g^*(0)$, $k_1$, $k_2$)=(3.31, 1.45, $1.83\times10^{-6}(h/0.7)^3{\rm Mpc}^{-3}{\rm mag}^{-1}$, $-21.61 + 5\log(h/0.7)$, 1.39, $-0.29$). The luminosity function is defined in terms of rest-frame $g-$band absolute magnitudes: we convert it to the observed $i$-band apparent magnitudes using the K-correction derived in Richards et al. (2006). Since the luminosity function was derived assuming $\Omega_M = 0.3$ and $\Omega_\Lambda = 0.7$, we adopt this set of values of cosmological parameters to compute the absolute magnitudes no matter what cosmologies we consider for the residual analysis.

In practice we use the cumulative luminosity function

$$\Phi(L) = \int_{\rm L}^{\infty} \phi\,(z_{\rm s}, L)\,dL, \tag{26}$$

to calculate the biased cross section

$$B\sigma = \int dX dY \frac{\Phi(L/\mu)}{L} = \int y \frac{\Phi(L/\mu)}{\Phi(L)} dy. \tag{27}$$

The integral is performed over the region where the flux ratio of faint to bright images is larger than $10^{-0.5}$. Furthermore, the SQLS quasar sample adopts quasars with Galactic extinction corrected (Schlegel et al. 1998) $i$-band magnitudes $15.0 \le i_{\rm cor} \le 19.1$, so we change the upper and lower limits of the cumulative luminosity function in Equation (27) correspondingly. Since lens models are circular, the integral is reduced to a one-dimensional one.

In addition, $\mu$ is taken to be the magnification of the brighter image depending on the SDSS quasar target selection method. The SDSS quasar target selection in Richards et al. (2002) used the Point Spread Function (PSF) for the magnitude limit. When the image separation is larger than $\sim 6$ arcsec, the PSF magnitude of the targeted quasar should be roughly equal to that of the brighter image (Oguri et al. 2006).

### 2.3 Lensing Probabilities

Consider the probability that a quasar at a certain redshift $z_{\rm s}$ is strongly lensed. The lensing efficiency with image separation larger than $\theta$ is given by

$$P(>\theta; z_{\rm s}) = \int_0^{z_{\rm s}} (1+z)^3 \frac{dD_{\rm L}}{dz} \int_{M(\theta)}^{\infty} \frac{dn}{dM} B\sigma dM, \tag{28}$$

where $B\sigma$ is the biased cross section and $D_{\rm L}$ is the proper distance from the observer to the lens object. The lower limit of the second integral $M(\theta)$ is the mass of a lens with an image separation $\theta$ at a given redshift $z$. Calculations show that the lowest mass of $M(\theta)$ capable of producing a separation of 10 arcsec is on the order of $10^{14}\ h^{-1}\ M_\odot$ in the context of this paper. The mass function of dark matter halos, $dn/dM$, is given by

$$\frac{dn}{dM} = -\frac{\rho_0}{M}\sqrt{\frac{2}{\pi}}\frac{\delta_c(z)}{\Delta^2}\frac{d\Delta}{dM}\exp\left[-\frac{\delta_c^2(z)}{\Delta^2}\right], \tag{29}$$

where $\Delta^2 = \Delta^2(M, z=0)$ is the present variance of fluctuations in a sphere containing a mean mass $M$ and $\delta_c(z)$ is the density threshold for spherical collapse by redshift $z$ (Li & Ostriker 2002).

The approximation of the redshift distribution of quasars is a Gaussian distribution and the results using these approximations agree well with those obtained by fully taking account of the observed redshift and magnitude distributions (Oguri & Keeton 2004).

$$p(z_{\rm s})dz_{\rm s} = \frac{1}{1.21}\exp\left[-\frac{(z_{\rm s}-1.45)^2}{2\times(0.55)^2}\right]dz_{\rm s}, \qquad 0.6 < z_{\rm s} < 2.3\,. \tag{30}$$

Hence the lensing probability with image separation larger than $\theta$ is

$$P(>\theta) = \int_{0.6}^{2.2} p(z_{\rm s}) dz_{\rm s} P(>\theta; z_{\rm s}). \quad (31)$$

## 3 RESULTS

### 3.1 Dependence on BCGs

We change the mass ratio of BCGs to their host dark matter halos to examine how the corresponding lensing probabilities vary. First, we take the mass of BCGs to be a fixed fraction of their host halos, i.e. $M_{\rm b}/M$ is a constant value regardless of the mass of host halos and calculate the lensing probability. Then we can plot the lensing probability as a function of $M_{\rm b}/M$, as shown in Figure 1. In this example, we adopt the $\Lambda$CDM1 cosmology, place the sources at redshift $z_{\rm s} = 1.5$ and compute the probability for image separations larger than $15''$, which is close to that of the discovered large-separation lensed quasar SDSS J1004+4112 with a splitting of $\theta = 14.7''$ (Inada et al. 2003) and also for image separations larger than $10''$, $20''$ and $25''$.

As we change the mass ratio $M_{\rm b}/M$, the corresponding variance tendencies of the total lensing probabilities are similar in the four situations where image separations are larger than $10''$, $15''$, $20''$ and $25''$. For $M_{\rm b}/M \to 0$, we recover the NFW case. As mass ratio $M_{\rm b}/M$ increases, the total lensing probability rises in all the four cases with different image separations. The significant dependence of lensing probability on the varying distribution of this mass ratio indicates that it might not be appropriate to assume a fixed mass ratio regardless of the mass of dark matter halos, especially for gravitational lensing on cluster scales (see Fig. 2). We will develop discussions on this issue in the second part of Section 3.

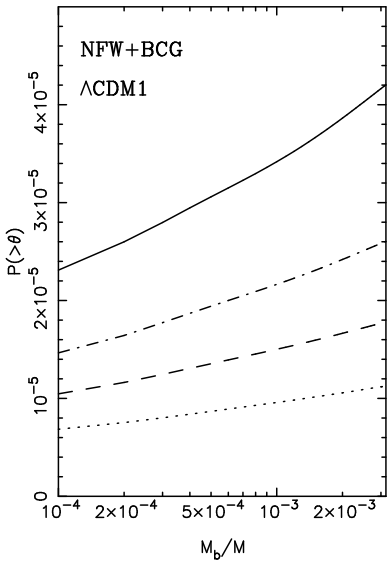


**Fig. 1** Predicted lensing probabilities of lensed quasars with separation $\theta > 10''$ (*solid* line), $\theta > 15''$ (*dot-dashed* line), $\theta > 20''$ (*dashed* line) and $\theta > 25''$ (*dotted* line) as a function of mass ratio of BCGs to their NFW-profiled host dark matter halos, $M_{\rm b}/M$, in $\Lambda$CDM1 cosmology. The lens is modeled as an NFW-profiled dark matter halo with a truncated SIS representing the BCG in its potential center.

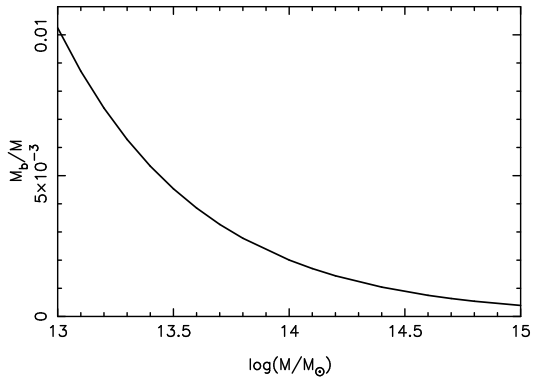


**Fig. 2** Mass ratio of the BCG to its host dark halo $M_{\rm b}/M$ as a function of the mass of host halo, $M$, according to Eq. (1) (Wang & Jing 2010).

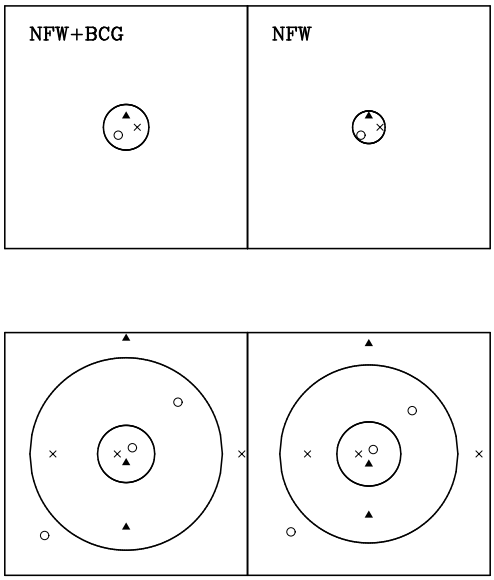


**Fig. 3** Caustics and critical curves for a typical cluster which consists of NFW-profiled pure dark matter with mass $M = 4.5 \times 10^{14}\ h^{-1}\ M_{\odot}$ at redshift $z = 1.0$ and for the same cluster with a BCG in its potential center. The top panels show the source planes and the bottom panels show the corresponding image planes.

In addition, working in dimensionless coordinates of the lens and the source planes, we calculate the critical curves and caustics for a typical cluster consisting of NFW-profiled pure dark matter with mass $M = 4.5 \times 10^{14}\ h^{-1}\ M_{\odot}$, which is the median value for the cluster lens sample (Hennawi et al. 2007a) at redshift $z = 1.0$. Furthermore, we also work out the corresponding critical curves and caustics of the cluster which include a BCG (modified as a truncated SIS) in its gravitational potential center. The results are shown in Figure 3. It can be seen that the baryonic matter can significantly

enhance the cross section for a single cluster. This is mainly because the cross section is sensitive to the inner slope and the addition of the BCG increases the inner slope and thus the cross section.

### 3.2 Statistics of Lensing Probabilities

We consider the full influences of BCGs and the redshift distribution of source quasars to compute cumulative lensing probabilities of large-separation lensed quasars for the SQLS quasar sample. The first important result is that BCGs located in the dark matter halos can dramatically enhance the lensing probability of large-separation quasar lenses, compared to pure dark matter clusters of NFW profiles. The total enhancement is a factor of $2 \sim 3$ among image separations $10'' < \theta < 30''$. This is consistent with the previous work from Oguri & Keeton (2004) and Hennawi et al. (2007b). Oguri & Keeton (2004) pointed out that for pure dark matter halos, the triaxial model predicted larger lensing probabilities for multiply-imaged quasars with an enhancement of a factor of $2 \sim 4$ over a spherical NFW model. Given these findings, for NFW-profiled dark matter halos, both triaxiality and BCGs enhance the overall lensing probability to the same degree. Hennawi et al. (2007b) showed that BCGs increased the lensing probability by $50\%$ and they used full ray-tracing simulations to calculate the number of multiply-imaged quasars by cluster-sized pure dark matter halos versus clusters including BCGs. Another interesting result is that the redshift distribution of quasars has a small effect on the whole lensing probability. Moreover, the evolution of the BCG-to-host mass ratio with redshift extending to $z \sim 1$ also has a small influence on lensing probabilities. However, the varying distribution of the mass ratio influences the lensing efficiency to a non-negligible extent, when compared to the mass ratio taken to be a fixed fraction regardless of the mass of dark matter halos as Hennawi et al. (2007b) and Li et al. (2007) did.

Many studies of clusters of galaxies preferred the NFW density profile (e.g., Comerford et al. 2006; Voigt & Fabian 2006; Sommer-Larsen & Limousin 2010) and we also adopt it as the profile of dark matter halos, but our study shows that the effect of BCGs cannot be ignored, as shown in Figures 1 and 4.

We integrate over a redshift distribution as in Equation (31) and consider the masses of BCGs as in Equation (1). Note that the mass ratios of BCGs to their host halos are not a constant value, see Figure 2. We calculate the lensing probabilities of large-separation lensed quasars in the $\Lambda$CDM1 cosmology with and without considering the total effects of BCGs. The expected cumulative number, $N$, of quasar lenses for the SQLS sample from DR5 is shown as a function of separation $\theta$ in Figure 4. From the figure, we can see that the expected numbers of quasar lenses with separation $\theta > 10''$ in the SQLS sample from DR5 which contains 36 287 quasars are $1.22$ for the $\Lambda$CDM1 cosmological model and $0.73$ for $10'' < \theta < 20''$, which are consistent with the only observed quasar lens SDSS J1004+4112 with $\theta = 14.7''$ in the complete sample. However, for the WMAP7 cosmology, the predicted numbers reduce to $0.47$ for $\theta > 10''$ and $0.33$ for $10'' < \theta < 20''$.

We also calculate the dependence of lensing probabilities on the redshift of the source quasars. One interesting result is that the effect of the redshift distribution of the source quasars on the whole lensing probability is less than several percent compared to all the sources being placed at redshift $1.5$. The small effect is mainly because the redshift distribution is a Gaussian function and the mean value of redshifts is $1.5$ (a standard deviation of $0.55$), which means most of the source quasars are at redshift $z_{\rm s} = 1.5$. Given this knowledge, we hereafter place all the quasars at $z_{\rm s} = 1.5$. Note that the lensing probabilities are in fact very sensitive to the redshift of the source quasars. We place all the quasars at the same redshift instead of considering their redshift distribution and calculate the lensing probability of image separation larger than $15''$ in the $\Lambda$CDM1 cosmology. Roughly, the probability increases as the sources are placed at higher redshift as expected. Moreover, the lensing probability of image separation larger than $15''$ for all quasars fixed at redshift $z_{\rm s} = 2.0$ is about two times that of all quasars fixed at redshift $z_{\rm s} = 1.5$. Bearing these in mind, it is very important to identify the median value of the quasar redshift distribution.

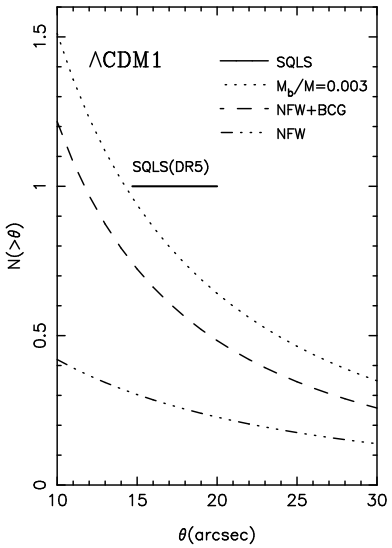


**Fig. 4** Theoretical cumulative number of large-separation lensed quasars as a function of image separation $\theta$ for the SQLS sample from SDSS DR5 in the ΛCDM1 cosmology. The heavy solid line shows the only observed large-separation cluster lens SDSS J1004+4112 of $\theta = 14.7''$ in the complete quasar sample. The dashed line and the dash-dotted line show the results for the NFW+BCG and the NFW lens models, respectively. As a comparison, the dotted line shows the results for the NFW+BCG lens model where the mass ratio of BCGs to their host halos is a constant value ($M_{\rm b}/M = 0.003$) regardless of the mass of host dark matter halos.

An important result is that the distribution of the mass ratio of BCGs to their host halos according to Equation (1) can reduce the cumulative lensing probability by $20\%$, when compared to assuming the mass ratio to be a fixed fraction of $0.003$ as Hennawi et al. (2007b) and Li et al. (2007) did; thus the effect of the distribution of mass ratio on the lensing probability cannot be ignored.

Figure 2 shows the mass ratio of BCGs to their host halos as a function of the mass of host halos. On cluster scales, the mass ratio $M_{\rm b}/M$ roughly reduces as the mass $M$ of the host halo increases. When the mass ratio $M_{\rm b}/M$ is $0.003$, it requires the host halo to have a corresponding mass of about $4 \times 10^{13}\ h^{-1}\ M_{\odot}$. For a dark matter halo with a mass more than that, the mass ratio is less than $0.003$ as can be seen from Figure 2, which means that the mass of a massive BCG in the innermost region is actually much less than $0.003M$ and the lensing rate is expected to be reduced compared to a fixed mass ratio of $0.003$. Moreover, for dark matter halos with masses more than several $10^{14}\ h^{-1}\ M_{\odot}$ which contribute the most to the large-separation lenses, the mass ratio is only $0.001$ or even less. Armed with the knowledge that lensing probability is very sensitive to the mass ratio in the first part of Section 3, especially to those less than 0.001 and that for wide-separation lenses, large mass dark matter halos contribute the most to lensing probabilities, so we cannot suppose the mass ratio of BCGs to their host dark halos to be a fixed fraction. In particular, we cannot assume the mass ratio to be a constant value of 0.003 since it overestimates the mass of BCGs and artificially enhances the lensing probability. Figure 4 shows the cumulative lensing probabilities as a function of image separation $\theta$ for considering the varying distribution of mass ratio and for a constant mass ratio $M_{\rm b}/M = 0.003$. In this example, we place all the quasar sources at redshift $z_{\rm s} = 1.5$ and still adopt the ΛCDM1 cosmology. We can see that, on average, lensing probabilities are reduced by $20\%$ when we take into account the distribution of mass ratio from

assuming a fixed ratio $M_{\rm b}/M = 0.003$. Therefore, the distribution of mass ratio of BCGs to their host halos according to Equation (1) has a non-negligible effect on lensing probabilities and is very important in the quantification of the effects of BCGs on lensing probabilities.

Finally, we calculate the effects of the evolution of BCG-to-host mass ratios with redshift on the lensing efficiency. This time, we still place all the quasars at redshift $z_{\rm s} = 1.5$ and work in the $\Lambda$CDM1 cosmology. It is feasible to take into account the evolution of BCGs out to redshift $0.83$ as described in the evolution model and not to consider the evolution beyond redshift $0.83$ in this example where the sources are set at $z_{\rm s} = 1.5$. The lensing probability peaks when lenses are at redshift $z = 0.5$ and lenses with redshift $0.3 < z < 0.6$ contribute more than $90\%$ of the total lensing probability. Our calculations show that the evolution of BCGs with redshift reduces the lensing efficiency by about $3\%$. One explanation for the small effect of the evolution of BCGs with redshift on lensing efficiency is that since we are concerned with large-separation images which are believed to be produced by high mass clusters with massive BCGs, the mass ratio of BCGs to their host halos towards the high mass end does not change much out to redshift 1.5 (Wang & Jing 2010). However, more quasars at higher redshifts will be observed in the future and the mass ratios of BCGs and their host halos on cluster scales are larger at high redshift (Behroozi et al. 2010), so the evolution of BCGs with redshift should have a more significant effect on the lensing efficiency at high redshifts.

### 3.3 Cosmological Dependence

We also calculate the lensing probability in the cosmology derived from the most recent seven-year WMAP data (WMAP7 cosmological model) and in the WMAP3 cosmological model.

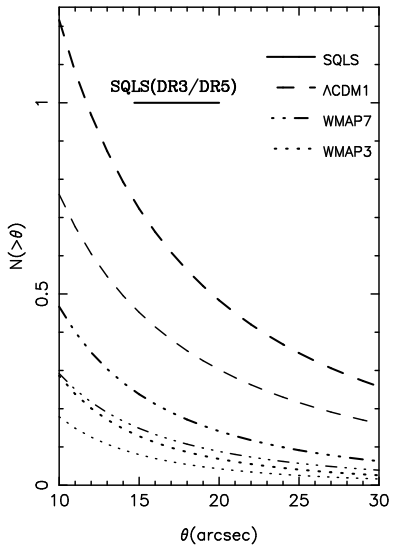


**Fig. 5** Predicted cumulative numbers of large-separation lensed quasars as a function of image separation $\theta$ in the $\Lambda$CDM1, WMAP3 and WMAP7 cosmologies. The heavy solid line shows the only observed large-separation cluster lens SDSS J1004+4112 in the complete SQLS quasar sample from SDSS DR3 or DR5 (both contain only one lens for large-separation). The thick lines are predictions for the SQLS sample from DR5 with 36 287 quasars and the thin lines are for the SQLS sample from DR3 with 22 683 quasars.

Figure 5 shows the cumulative number of lens systems as a function of image separation $\theta$ for those cosmologies. In this endeavor, we still place all the quasars at redshift $z_{\rm s} = 1.5$. The predicted numbers of lensed quasars in the SQLS sample from DR5 with image separation $\theta > 10''$ are $0.29$ in the WMAP3 model and $0.47$ in the WMAP7 model, much less than that in the $\Lambda$CDM1 cosmology, which is $1.22$. Also, the expected numbers of lensed quasars for the sample with $10'' < \theta < 20''$ are $0.10$, $0.33$ and $0.73$, respectively for WMAP3, WMAP7 and $\Lambda$CDM1. In the SQLS samples from DR3 and DR5, each has one lensed quasar with separation $10'' < \theta < 20''$. On the whole, the ratio of lensing efficiencies between WMAP3 and $\Lambda$CDM1 is $1/5 \sim 1/10$ for $10'' < \theta < 20''$ and $1/3 \sim 1/4$ for WMAP7 over $\Lambda$CDM1. The reductions are mainly because of the smaller $\sigma_8$ ($0.801$ in WMAP7 cosmology and $0.762$ in WMAP3 cosmology, but $0.9$ in $\Lambda$CDM1 model) and lower $\Omega_{\rm M}$ ($0.266$ in WMAP7 and $0.238$ in WMAP3, but $0.3$ in $\Lambda$CDM1 model).

## 4 SUMMARY AND DISCUSSION

In this paper, we calculate the expected number of multiply-imaged quasars lensed by clusters of galaxies in the SQLS sample from SDSS DR5, which is a complete well-defined sample for the statistical analysis of quasar lenses. We work in three cosmologies, the $\Lambda$CDM1 cosmology and two cosmologies derived from WMAP three-year and seven-year data. Previous studies were made by Hennawi et al. (2007b) and Li et al. (2007). Our work extends their studies by making a detailed analysis of the effects of BCGs on gravitational lensing probabilities, by adopting the most recent cosmology determined by WMAP data and by using a complete sample suitable for statistical analysis.

In the frame of the $\Lambda$CDM1 cosmological model in the paper, a spherical NFW-profiled dark halo with a BCG (modified as a truncated SIS) located in its center can explain strong gravitational lensing, in particular lensing probabilities. Pure dark matter halos with a circular NFW density profile have a low efficiency in producing lens systems, but the observed baryonic matter, here characterized by BCGs, can enhance the lensing probability by a factor of $2 \sim 3$. This is equivalent to the enhancement made by triaxiality of dark matter halos, which is approximately $2 \sim 4$; thus BCGs cannot be ignored in calculating the lensing efficiencies. Moreover, the lensing rate predicted by our lens model considering both dark matter and baryonic matter, or say circular NFW+BCG, matches with the observations when we adopt the SQLS sample from DR5. The predicted number of lensed quasars in $\Lambda$CDM1 cosmology with image separations between $10''$ and $20''$ is $0.73$, which is consistent with the only observed cluster lens with an image separation of $14.7''$ in the complete quasar sample. This number is $0.33$ in WMAP7 cosmology, which is also reasonable except that a higher $\sigma_8$ is preferable. Note that the present size of a strong lensing sample suitable for statistics is too small, which limits the actual precisions for constraining the relevant physical parameters. However, future observations will enlarge the quasar sample and our methods are useful for that.

The effects of BCGs on strong lensing are actually less dramatic than previous studies expected. The dependence of the mass ratio of BCGs to their host halos on dark matter halo masses reduces the lensing rate by $20\%$ from assuming a fixed mass ratio ($M_{\rm b}/M = 0.003$) (adopted by Hennawi et al. 2007b and Li et al. 2007) of BCGs to their NFW-profiled host halos. In fact, for large-separation lenses which are produced by massive clusters of galaxies, the mass ratios are around $0.001$ or even less. On cluster scales, the mass ratio $M_{\rm b}/M$ generally reduces as the mass $M$ of host halos increases as shown in Figure 2 and the lensing rate reduces as the mass ratio decreases, so we should handle the mass ratio carefully. As our results show, a decrease of $20\%$ in lensing probabilities for considering the distribution of mass ratio versus setting all BCGs to be a fixed fraction of the mass of spherical NFW-profiled host halos, the enhancement of the lensing efficiency by BCGs in the center of dark matter halos should be less than $50\%$ in Hennawi et al. (2007b).

Our predicted numbers of large-separation multiply-imaged quasars for the SQLS sample from DR5 are lower than those given by Li et al. (2007) roughly by a factor of $2$ in the $\Lambda$CDM1 cosmology

and a factor of $1.5$ in the WMAP3 cosmology. The difference is mainly due to three reasons. First, Li et al. (2007) adopted an elliptical dark matter halo model, while we use a spherical NFW model. Oguri & Keeton (2004) concluded that the ellipticity of dark matter halos enhanced the lensing rate by a factor of four for the spherical NFW model and their work did not account for the baryonic matter. The ellipticity of dark matter halos should have a smaller effect on lensing efficiencies when considering baryons in the inner most regions of halos than the case without taking into account baryons, because our results show that baryons and the ellipticity of halos affect lensing rate at the same level, the former by a factor of $2 \sim 3$ and the latter by a factor of $2 \sim 4$. Another reason for the difference is that Li et al. (2007) adopted a higher and constant mass ratio ($0.003$) of BCGs for their host halos, whereas we consider the mass ratio distribution as a function of the mass of host dark matter halos. The third reason is that the quasar sample (containing $46\,420$ quasars) they used was $25\%$ larger than the SQLS sample from DR5 that we use. Our results are different from those given by Hennawi et al. (2007b) roughly for the same reasons. In addition, we point out that they used a different cosmology so there are more factors.

We show clearly that the NFW+BCG model we adopt can be improved in several ways. First, we assume a spherical NFW density profile for dark matter halos but recent simulations prefer a triaxial profile. Since the triaxiality has a significant effect on the lensing probabilities, this should be included properly. Secondly, we consider that the cluster concentration is the mean concentration $c_{\rm vir}(M)$ as a function of mass of the dark matter halos, but we do not consider the distribution of the $c_{\rm vir}/c_{\rm vir}(M)$. However, Hennawi et al. (2007b) pointed out that simply computing the mean concentration in mass bins would be sensitive to outliers and very noisy at the high mass end where we have few clusters. Another aspect that needs improving is that there is a scatter, which was described with a Gaussian function in Wang & Jing (2010), of the mass of BCGs at a given mass $M$ of their host halos, but we do not implement the distribution.

Finally, although the circular NFW+BCG model can, to some extent, explain large-separation lensed quasars in the SQLS sample, we still have several problems that require further study. First, the spherical density profile can well explain the lensing probability of image separations of quasar lenses, but it cannot account for image multiplicities which are believed to be the result of the triaxiality. We are preparing another paper on it. Another important factor that needs to be considered is the substructures of galaxy clusters. Oguri (2006) predicted that $10\% \sim 20\%$ of lenses should be caused by the subhalo population (satellite galaxies instead of central galaxies). However, we do not take into account how substructures affect image multiplicities. The third fact is the lack of knowledge of BCGs. Although we suppose that each BCG is located in the potential center of its host halo, they might change their positions when two clusters merge, which may also lead to interesting lensing events. However, these intriguing issues are beyond the scope of this paper and they can be considered in the subsequent work.

**Acknowledgements** HQ thanks Li-Xin Li, Dan-Dan Xu, Huan-Yuan Shan, and Lan Wang for useful discussions. This work was supported by the National Natural Science Foundation of China (Grant No. 11073023) and the National Basic Research Program of China (973 Program; Grant No. 2009CB24901).

## References

Ahn, E.-J., Bertone, G., Merritt, D., & Zhang, P. 2007, Phys. Rev. D, 76, 023517
Bartelmann, M., Huss, A., Colberg, J. M., Jenkins, A., & Pearce, F. R. 1998, A&A, 330, 1
Bartelmann, M., Meneghetti, M., Perrotta, F., Baccigalupi, C., & Moscardini, L. 2003, A&A, 409, 449
Behroozi, P. S., Conroy, C., & Wechsler, R. H. 2010, ApJ, 717, 379
Bowman, J. D., Hewitt, J. N., & Kiger, J. R. 2004, ApJ, 617, 81
Boyle, B. J., Shanks, T., Croom, S. M., et al. 2000, MNRAS, 317, 1014

Bradač, M., Schrabback, T., Erben, T., et al. 2008, ApJ, 681, 187
Broadhurst, T., Takada, M., Umetsu, K., et al. 2005, ApJ, 619, L143
Bullock, J. S., Kolatt, T. S., Sigad, Y., et al. 2001, MNRAS, 321, 559
Chen, D.-M. 2003a, ApJ, 587, L55
Chen, D.-M. 2003b, A&A, 397, 415
Chen, D.-M. 2004, A&A, 418, 387
Comerford, J. M., Meneghetti, M., Bartelmann, M., & Schirmer, M. 2006, ApJ, 642, 39
Croom, S. M., Smith, R. J., Boyle, B. J., et al. 2004, MNRAS, 349, 1397
Gavazzi, G., Donati, A., Cucciati, O., et al. 2005, A&A, 430, 411
Hennawi, J. F., Dalal, N., & Bode, P. 2007a, ApJ, 654, 93
Hennawi, J. F., Dalal, N., Bode, P., & Ostriker, J. P. 2007b, ApJ, 654, 714
Huterer, D., & Ma, C.-P. 2004, ApJ, 600, L7
Inada, N., Becker, R. H., Burles, S., et al. 2003, AJ, 126, 666
Inada, N., Oguri, M., Morokuma, T., et al. 2006, ApJ, 653, L97
Keeton, C. R., & Madau, P. 2001, ApJ, 549, L25
Kochanek, C. S. 1995, ApJ, 453, 545
Kochanek, C. S. 2002, ApJ, 578, 25
Kochanek, C. S., & White, M. 2000, ApJ, 543, 514
Kuhlen, M., Keeton, C. R., & Madau, P. 2004, ApJ, 601, 104
Li, G. L., Mao, S., Jing, Y. P., Lin, W. P., & Oguri, M. 2007, MNRAS, 378, 469
Li, L.-X., & Ostriker, J. P. 2002, ApJ, 566, 652
Li, N., & Chen, D.-M. 2009, RAA (Research in Astronomy and Astrophysics), 9, 1173
Limousin, M., Richard, J., Kneib, J.-P., et al. 2008, A&A, 489, 23
Lopes, A. M., & Miller, L. 2004, MNRAS, 348, 519
Lynds, R., & Petrosian, V. 1986, in Bulletin of the American Astronomical Society, 18, 1014
Mao, S., Witt, H. J., & Koopmans, L. V. E. 2001, MNRAS, 323, 301
Mitchell, J. L., Keeton, C. R., Frieman, J. A., & Sheth, R. K. 2005, ApJ, 622, 81
Mortlock, D. J., & Webster, R. L. 2000a, MNRAS, 319, 860
Mortlock, D. J., & Webster, R. L. 2000b, MNRAS, 319, 872
Nakamura, T. T., & Suto, Y. 1997, Progress of Theoretical Physics, 97, 49
Narayan, R., & White, S. D. M. 1988, MNRAS, 231, 97P
Navarro, J. F., Frenk, C. S., & White, S. D. M. 1997, ApJ, 490, 493
Newman, A. B., Treu, T., Ellis, R. S., et al. 2009, ApJ, 706, 1078
Oguri, M. 2006, MNRAS, 367, 1241
Oguri, M., Inada, N., Pindor, B., et al. 2006, AJ, 132, 999
Oguri, M., Inada, N., Strauss, M. A., et al. 2008, AJ, 135, 512
Oguri, M., & Keeton, C. R. 2004, ApJ, 610, 663
Oguri, M., Lee, J., & Suto, Y. 2003, ApJ, 599, 7
Oguri, M., Taruya, A., Suto, Y., & Turner, E. L. 2002, ApJ, 568, 488
Paczynski, B. 1987, Nature, 325, 572
Porciani, C., & Madau, P. 2001, ApJ, 548, 522
Richards, G. T., Croom, S. M., Anderson, S. F., et al. 2005, MNRAS, 360, 839
Richards, G. T., Fan, X., Newberg, H. J., et al. 2002, AJ, 123, 2945
Richards, G. T., Strauss, M. A., Fan, X., et al. 2006, AJ, 131, 2766
Sarbu, N., Rusin, D., & Ma, C.-P. 2001, ApJ, 561, L147
Schlegel, D. J., Finkbeiner, D. P., & Davis, M. 1998, ApJ, 500, 525
Schmidt, R. W., & Allen, S. W. 2007, MNRAS, 379, 209
Smith, R. J., Croom, S. M., Boyle, B. J., et al. 2005, MNRAS, 359, 57

Sommer-Larsen, J., & Limousin, M. 2010, MNRAS, 408, 1998
Soucail, G., Fort, B., Mellier, Y., & Picat, J. P. 1987, A&A, 172, L14
Takahashi, R., & Chiba, T. 2001, ApJ, 563, 489
Tu, H., Limousin, M., Fort, B., et al. 2008, MNRAS, 386, 1169
Turner, E. L., Ostriker, J. P., & Gott, J. R., III 1984, ApJ, 284, 1
Umetsu, K., & Broadhurst, T. 2008, ApJ, 684, 177
Voigt, L. M., & Fabian, A. C. 2006, MNRAS, 368, 518
Walsh, D., Carswell, R. F., & Weymann, R. J. 1979, Nature, 279, 381
Wambsganss, J., Cen, R., Ostriker, J. P., & Turner, E. L. 1995, Science, 268, 274
Wang, L., & Jing, Y. P. 2010, MNRAS, 402, 1796
Wyithe, J. S. B., Turner, E. L., & Spergel, D. N. 2001, ApJ, 555, 504
Zappacosta, L., Buote, D. A., Gastaldello, F., et al. 2006, ApJ, 650, 777